



A Pseudo 3D seismic refraction tomography for exploring archaeological structures Una pseudo tomografía 3D de refracción sísmica para explorar estructuras arqueológicas

Cárdenas-Soto Martín

Universidad Nacional Autónoma de México

Facultad de Ingeniería, Geofísica

E-mail: martinc@unam.mx

<https://orcid.org/0000-0002-6586-469X>

Gámez-Lindoro José Antonio

Universidad Nacional Autónoma de México

Facultad de Ingeniería, Geofísica

E-mail: king-nido@hotmail.com

<https://orcid.org/0000-0002-7367-2807>

Peña-Gaspar Valeria

Universidad Nacional Autónoma de México

Facultad de Ingeniería, Geofísica

E-mail: valepega@unam.mx

<https://orcid.org/0000-0003-1203-3961>

Aguirre-Díaz Juan Pablo

Universidad Nacional Autónoma de México

Facultad de Ingeniería, Geofísica

E-mail: juan.aguirre@ingenieria.unam.edu

<https://orcid.org/0000-0003-2273-8412>

García-Serrano Alejandro

Universidad Nacional Autónoma de México

Facultad de Ingeniería, Geofísica

E-mail: agarcia@unam.mx

<https://orcid.org/0000-0002-0677-0829>

Abstract

In the seismic refraction method, refracted waves provide the velocity and irregularity of the substratum. In this study, we took advantage of this method to construct 3D images of the refractor subsurface for two rectangular arrays of sources and receivers. The procedure consists of fitting a straight line to the refracted arrival times that pass through each of the cells that discretize the study surface. The slope inverse is the P-wave velocity, and the intercept time allows us to estimate the substratum depth. We applied this method to two archaeological zones where it was necessary to know the structure of the subsoil velocity and the possible presence of anomalies associated with buried constructions. The results show velocity anomalies related to buried structures and lateral discontinuities due to changes in the refractor layer composition. At the site of Plazuelas, Guanajuato, the slope irregularity of this refractor indicates the unevenness of the ground that had to be filled for the Pyramid's construction. At the Xalasco site, Tlaxcala, impedance contrast is low, but lateral velocity variations show anthropogenic anomalies related to the distribution of remains of ceremonial archaeological foundations.

Keywords: Seismic refraction, seismic tomography, substratum, archaeology, 3D studies.

Resumen

En el método de refracción sísmica las ondas refractadas proveen la velocidad e irregularidad del substrato. En este estudio aprovechamos el principio de este método para construir imágenes 3D de la superficie refractora para dos arreglos rectangulares de fuentes y receptores. El procedimiento consiste en ajustar los tiempos de arribo de las ondas refractadas que cruzan cada una de las celdas que discretizan la superficie de estudio. El inverso de la pendiente es la velocidad de onda compresional y el intercepto permite calcular la profundidad del substrato. Aplicamos este método a dos zonas arqueológicas donde se requería conocer la estructura de velocidad del subsuelo y la posible presencia de anomalías asociadas a construcciones enterradas. Los resultados muestran la presencia de anomalías de velocidad que se pueden relacionar con estructuras enterradas y discontinuidades laterales por cambios en la composición de los materiales del substrato refractor. En el sitio de Plazuelas, Guanajuato, la irregularidad en la pendiente de este refractor indica el desnivel del terreno que tuvo que ser rellenado para la construcción de la Pirámide. En el sitio de Xalasco, Tlaxcala, el contraste de impedancia es bajo, pero las variaciones laterales de velocidad muestran anomalías de origen antropogénico que se pueden relacionar con estructuras arqueológicas de interés.

Descriptores: Refracción sísmica, tomografía sísmica, substrato, arqueología, estudios 3D.

INTRODUCTION

Seismic methods carry out the geophysical characterization of the mechanical properties of the subsoil. In the first meters of depth, seismic refraction is widely used to determine the velocities of compressive waves (V_p) and the thicknesses of shallow layers. The examination depth is limited by the presence of the higher velocity layer (in addition to the acquisition design), which may be of particular interest if its mechanical properties (velocities and elastic modules) classify it as the substratum. The seismic reflection method provides a better definition of the subsurface V_p structure; however, acquisition and processing are more expensive (Yilmaz, 2015). The characterization of the substratum allows to:

- a) Establish the parameters of the foundation design.
- b) Determine the local amplification effects for seismic microzonification purposes.
- c) Detect the presence of the impermeable layer in shallow aquifer studies.
- d) Establish the depth of study for the characterization of the Critical Zone (Brantley *et al.*, 2006).

The subsoil exploration is also carried out by spectral analysis of surface waves produced during seismic surveys (active methods). The methods traditionally used are MASW (Park *et al.*, 1999; Xia *et al.*, 1999) and SASW (Nazarian, 1984; Nazarian and Desai, 1993), which provide representations of the shear wave velocity (V_s). The rise of seismic noise methods (passive methods) has made it possible to complement the active methods. Array stations methods as SPAC (Aki, 1957; Okada & Suto, 2003), ReMi (Louie, 2001), and Seismic Interferometry (e.g., Shapiro & Campillo, 2004; Shapiro *et al.*, 2019) take advantage of the stationarity of ambient seismic noise recorded at more than two stations to determine V_s and even reach greater depths. If we use seismic noise recorded in a single triaxial seismic station, the method of spectral ratios H/V (Nakamura, 1989; Lermo & Chávez, 1994) could establish a first approximation of the depth of the substructure (e.g., García-Jerez *et al.*, 2006; Hellel *et al.*, 2019).

The indicated methods acceptably carry out the delineation of the substratum. The 3D representation of the subsoil velocity structure can be established by massive data acquisition in a single method or the combination of active and passive methods (e.g., Cardenas *et al.*, 2016, 2020; Hussain *et al.*, 2019; Chávez *et al.*, 2021; Martorana & Capizzi, 2020). Whether 2D or 3D representation, data acquisition must be performed above the study target. An alternative to avoid invading the surface to be explored is the Seismic Interferometry method, which obtains

the medium properties between pairs of stations. If an extensive array of receptors surrounds the area to be explored, we can perform a V_s tomography of the subsoil (e.g., Argote *et al.*, 2020; Cardenas *et al.*, 2020, 2021). A limitation of this method is that it requires an azimuthal distribution of noise sources and a dispersive medium to obtain an adequate distribution of velocities (Forghani & Snieder, 2010). However, different processing techniques have been implemented to mitigate the lighting of noise sources and highlight the dispersive character (Balestrini *et al.*, 2020; Liu *et al.*, 2021). The processing cost translates into more elaborate procedures with greater time consumption in quality control steps and seismic noise recording time.

A procedure not yet fully explored is the refraction tomography of sources and receptors on the surface (RTSRS). This method could provide a 2D image of the subsurface P-wave velocity distribution in two stages. The first is to identify the arrival times of the refracted waves, and the second is to solve the velocity and depth of the refractor in a discretized surface. Geophysical engineering students of UNAM have carried out this type of experiment to comply with field practices. In this type of experiment, seismic records contain primary arrivals that result from a combination of direct, refracted, and reflected waves. The results obtained so far show V_p subsoil images indicating lateral discontinuities due to subsoil composition (Ramos, 2015; Gamez, 2021). However, these images cannot be assigned an investigation depth because travel time first arrivals are mixed in the data inversion.

This study explores the RTSRS method, whose acquisition design raises the following questions: can refracted waves detect lateral variations with sufficient velocity contrast to recognize anthropogenic irregularities in the subsoil? Furthermore, the depth of the irregularities is related to the depth predicted by the linear model of the P-wave arrival times? The objective is to determine anomalies of interest and the refracting sublayer shape and depth under two archaeological structures. In the first stage, we explore the subsoil through seismic refraction sections along the lines that make up quadrangular arrays surrounding the structures. Subsequently, we describe the RTSRS method and analyze the tomography refraction images according to the substratum irregularity. Finally, we discuss our results and indicate the advantages and limitations of the method.

STUDY ZONES AND DATA ACQUISITION

We investigate two archaeological sites. The first one corresponds to the area called Plazuelas in the municipi-

pality of Pénjamo, State of Guanajuato. In this area, there are several buildings, but the most important corresponds to the building known as Casas Tapadas, where we carried out the study. The construction consists of a large rectangular platform on which four pyramidal bases were built for expansion. In the southern base of this structure, there are signs of leveling the land to preserve the building's horizontality when constructing one of the basements (Secretaría de Cultura/INAH, 2020). The surface land materials are made up of basaltic tuff and sandstone (Pérez *et al.*, 1999). It is worth mentioning that although another series of geophysical experiments have been carried out in the area (Morales *et al.*, 2015; Huerta, 2017; Rocha, 2017), none of them had been directed to explore the subsoil under the pyramid to know the conditions of ground leveling for its foundation.

Seismic experiments were carried out to study ground leveling conditions. For this purpose, 72 vertical geophones of 4.5 Hz were placed around the central pyramid with a spacing of 1.77 m forming a square arrangement of 32 m per side (Figure 1). By the percussion of a metal plate with a 12 lb sledgehammer, 16 seismic sources were produced distributed around the arrangement at one meter of separation of the geophones line. In each source point, five strokes were stacked whose values were recorded on six SEISTRONIX EX6 model seismographs. Figure 3a shows an example of the traces recorded for source 1, where the primary arrivals (direct and refracted waves) with arrival times no greater than 30 ms are clearly observed.

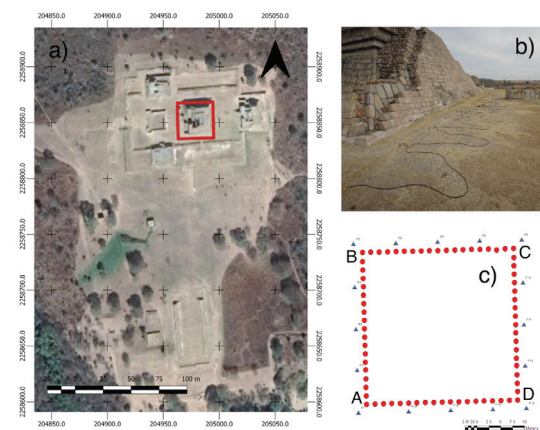


Figure 1. a) Location of the seismic survey within the archaeological zone of Plazuelas, b) image of a pyramid side and geophones line, c) geophones array (red circles) and points where the sources were generated (blue triangles). Capital letters indicate the sources of the seismic refraction profiles formed along the lines that define the geophones

The second site is located in the archaeological zone of Xalasco, municipality of Atltzayanca, Tlaxcala. There

are several pre-Hispanic sites in the area, some of which have been objects of archaeological and geophysical studies (Argote *et al.*, 2016; Juárez *et al.*, 2017). The selection site was in conjunction with INAH archaeologists to characterize what they believe may be a prehispanic construction of the Teotihuacan culture (Manzanilla & Bautista, 2019; López *et al.*, 2016). The study was carried out in an agricultural area consisting of soil deposits overhanging andesitic tuffs (Juárez *et al.*, 2017). In the acquisition of seismic data, 48 vertical geophones of 4.5 Hz with a separation of 5 m were used to form a square arrangement of 60 m per side. Like the previous experiment, 16 sources distributed around the arrangement were used (Figure 2). Figure 3b shows an example of the records produced by source 1. In this case, we observe that the refracted arrival times reach up to 150 ms on average; that is, we can infer that the subsurface velocity materials are lower than in the previous site.

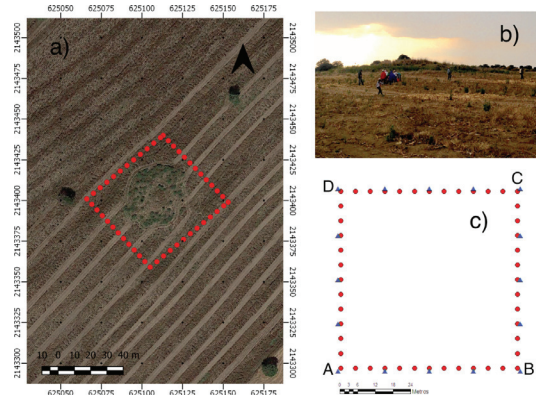


Figure 2. a) Location of the seismic survey within the archaeological zone of Xalasco, b) photograph of the site study appearance, c) geophones array (red circles), and points where the sources were generated (blue triangles). Capital letters indicate the sources of the seismic refraction profiles formed along the lines that define the geophones

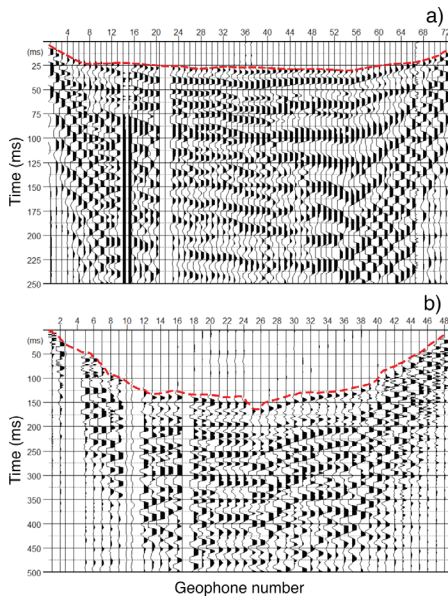


Figure 3. Example of recordings produced by a seismic source, a) Plazuelas site, b) Xalasco site. The dashed red lines indicate the first arrivals of the direct and refracted waves. On both sites, some channels did not operate

THE SEISMIC REFRACTION METHOD

The seismic refraction method is widely used to determine the compressional wave velocity structure of the subsoil. By recording direct and refracted arrival times along a linear array of receivers, travel-time curves are constructed as a function of distance. Figure 4 sketches the interpretation of those times by adjusting straight lines to the data; the slope of the direct arrivals defines the upper layer’s velocity, and the slope of the refracted arrivals determines the subjacent layer velocity. The travel time of a refracted wave (trajectory ABCD) can be represented by Equation 1, whose second term is the *y* intercept (*T_i*). The refractor depth (*h*) is determined from the *T_i* value once the layer and sub-layer velocities are determined. Using Equation 2, it is also possible to solve for *h* if we fix the distance at which the refracted arrivals begin to appear (crossover distance).

There are different methods to interpret the first arrivals represented in a travel-time plot. One of the first is the Generalized Reciprocal Method (Palmer, 1981), which is based on determining the arrival times of direct and reverse shots in pairs of receivers. Currently, traditional refraction processing has been replaced by tomography refraction. In this method, a subsurface structure model is constructed with the velocity variations produced by adjusting the travel times observed with those derived from the ray tracing (Sheehan *et al.*, 2005; Zelt *et al.*, 2013). According to the densi-

ty of selected arrival times, a detailed image of the 2D velocity structure can be built, where the anomalies produced by various discontinuities (faults, pipes, cavities, foundations, etc.) can be reasonably interpreted.

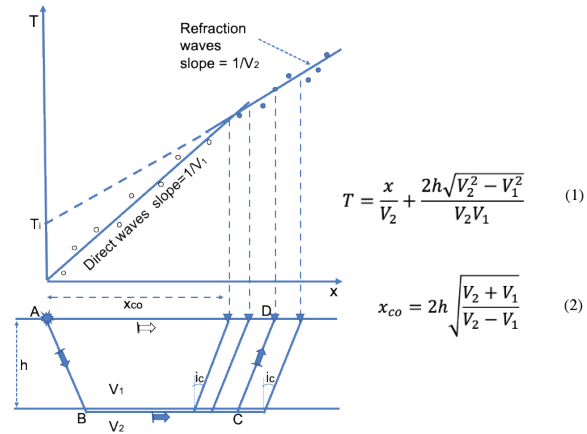


Figure 4. Interpretation scheme of direct (hollow circles) and refracted (solid circles) arrivals in the seismic refraction method. The travel time of a refractive wave (trajectory ABCD that emerges with a critical angle (*ic*) is represented by the equation of a straight line (Equation 1) whose *y* intercept time *T_i* (second term) allows to determine the refractor depth (*h*). The crossover distance (*x_{co}*) also allows to solve for *h*

SEISMIC REFRACTION PROFILES

Figure 5 shows the first arrivals of all seismic sections of each site. At the Plazuelas site (Figure 5a), we observe a large dispersion for direct and refracted arrivals. This dispersion indicates the substructure irregularity under the pyramid structure. The crossover distance at which the refracted arrivals begin to appear is 7.5 m. In comparison, the first arrivals at the Xalasco site (Figure 5b) follow an almost linear behavior. In the travel-time plot, we can identify the critical distance as approximately 20 m. The time arrivals slope reveals a low contrast of velocities between the refractor and the surface layer.

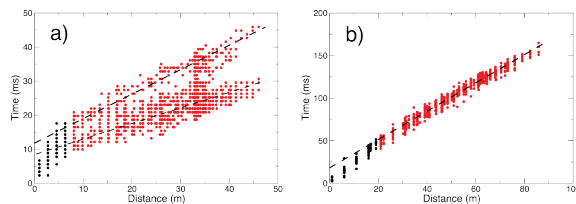


Figure 5. First arrival times as a function of the distance for the sites of: a) Plazuelas and b) Xalasco. The black circles represent the direct arrivals, and the red circles represent the refracted arrivals. The dashed black lines indicate the possible best fit of a line to the refracted arrivals

A first approach for identifying the basement under each structure is to analyze the seismic refraction sections (SRS). Since we have built quadrangular arrays, we can obtain four SRS along the receiver lines that make up each array. To do this, we process the first arrivals using the Zondst2D program (Kaminsky, 2015), which produces a tomography image by best fit of the observed travel times with those calculated from an initial velocity model. New travel times are produced from the updated model in each interaction until producing the best model with the minor fit error.

Figure 6a shows the SRS around the Pyramid of the Casas Tapadas site. Arrival times allow us to define a layer on an irregular sub-layer. Along the BC section, the layer has a thickness of 1m because the line is perpendicular to the lithological dip layers. In the other sections, the thickness is from 2 to 5 m. The velocity of the first layer is on average 800 m/s and the sub-layer 1400 m/s. Although the thicknesses at the ends of each section are interpolated (because refracted arrivals cannot be obtained at distances less than the critical distance), we observe a good agreement between the thicknesses of the surface layer obtained at the ends that join each section. The layer has a thickness of 2 m on the north side (Section B-C) and 5 m on the south side (Section D-A).

The SRS of the site Xalasco is shown in Figure 6b. The arrival times modeling allows us to determine a layer of an average thickness of 2.75 m with a velocity of 430 m/s overlaying to substratum of 500 m/s. The velocity contrast between the layer and the substratum is weak, as shown by the arrival times of Figure 5b; however, we can define the substratum irregularity such that the depth of the layer can be followed at the ends of each section.

PSEUDO SEISMIC REFRACTION TOMOGRAPHY

We now explore the refracted arrivals recorded in the closed array of receivers with a distribution of sources on the surface and surrounding the array (RTSRS method). In this case, the primary waves recorded can be direct arrivals or reflected at short distances or refracted at intermediate to long distances. The proposed acquisition geometry does not allow applying the classical interpretation of the refraction method to determine the velocity and depth refractor. However, as we observed in the previous section, the representation of these travel times in a time-distance graph permits identifying direct and refracted arrivals (Figure 5).

If the study area is discretized with cells proportional to the geophone separation, we can identify the source-receiver trajectories that cross each cell. The refracted arrivals of these trajectories can be used to determine the refractor velocity if we adjust these arrivals to the slope-intercept straight line form (Equation 1, Figure 4). Figure 7 shows a ray-tracing diagram due to three sources and twelve receivers, where the ray paths converge in a cell located at a depth where the wavefronts are refracted due to enough impedance velocity contrast. The representation of the slopes inverse (or velocities) for each cell will provide us with a pseudotomography of the velocity variations under the receiver array. The intercept time can be utilized to determine the refractor depth according to the second term of Equation 1. In this estimate, the top layer velocity (V_1) can be considered constant.

We have used the refracted arrivals of each site to create a pseudo-velocity tomography of the refractor substructure. The surface covered by the array was di-

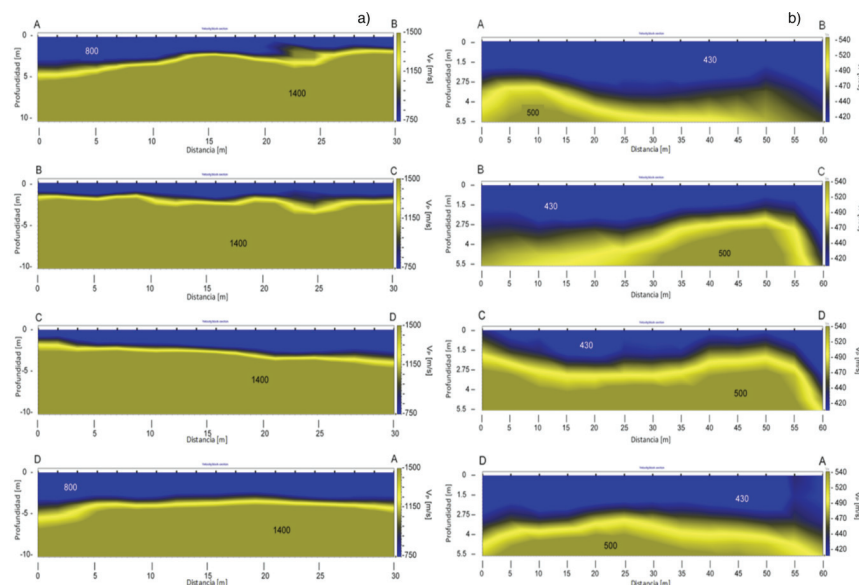


Figure 6. Seismic refractions sections obtained along the receiver lines that make up each array, a) Plazuelas site, b) site of Xalasco

vided into cells of 5 m per side, and we assign the refracted trajectories (travel times) to each cell to perform a nonlinear least-squares fit using the Marquardt-Levenberg algorithm (Williams & Kelley, 2019). The solution provides the refractor velocity (V_2) as the straight-line slope inverse (Equation 1). The intercept time allows calculating the refractor depth if we use the average velocity of the upper layer (V_1 ; given in the refraction sections) and V_2 estimated in each cell.

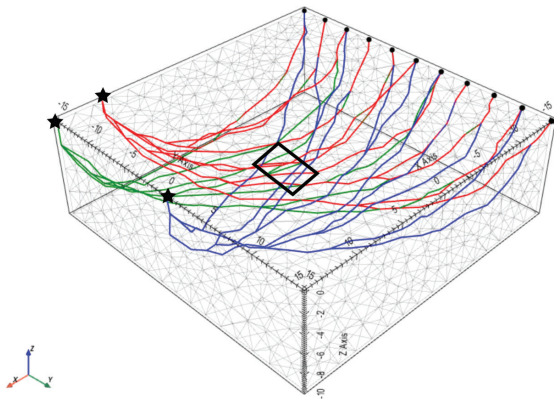


Figure 7. Ray path scheme (three sources and twelve receivers) in a 3D medium whose velocity increases with depth. The black rectangle indicates a cell where the refracted rays converge (modified from: https://www.pygimli.org/_examples_auto/2_seismics/plot_05_refraction_3D.html)

Figure 8a shows the results under the Pyramid of Casas Tapadas. The velocity distribution has values higher than 1500 m/s, in agreement with the substratum velocity resolved in the SRS of Figure 6a. Velocities larger than 2500 m/s are observed in the southern and southwest of the array, where depths are between 5 and 7 m. In the northern and northeast, we observe velocities are lower (1500 to 2500 m/s), and the depths are in the range of 2.5 to 5 m. We found that the depth values are consistent with those found in the SRS. The refractor layer is deeper at the southern part and shallower at the northern part. Figure 8b shows the error percentage quantified by the RMS of the calculated residuals in each cell. Practically the regression error is less than 0.3 %, indicating an acceptable best-fit of the arrival times.

According to the SRS results at the Xalasco site, tomography velocities are between 500 to 700 m/s with an average depth of 3 to 4 m (Figure 9a). The tomography image of Figure 9a shows that the lateral variation of velocities is very low. Velocities of 700 m/s up to 8 m deep can be highlighted as anomalies of interest. It is observed that the anomaly that is located on the southeast extreme (near Point B) is not solved in the refraction line BC (Figure 6b), which probably is due to the low contrast velocity between the top and bottom

layer. According to the residual RMS (Figure 9b), the zone with the most significant best-fit error is observed at the southwest. Both the high-velocity anomalies and the velocities on the Northern zone of the array can be considered reasonably resolved given that the RMS values are less than 0.5 %.

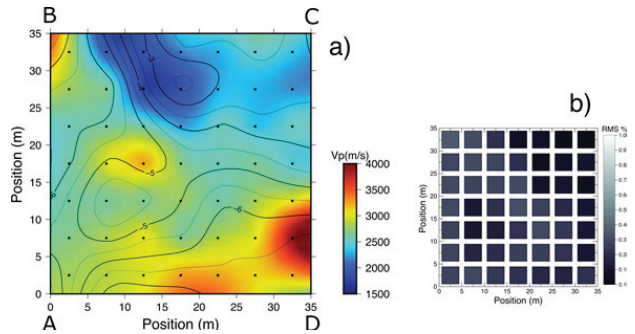


Figure 8. a) Pseudo seismic refraction tomography at Plazuelas site. The black lines represent the iso-depths of the refractor layer in meters. Black dots are the centers of cells, b) RMS residuals representation of travel times inversion in each cell

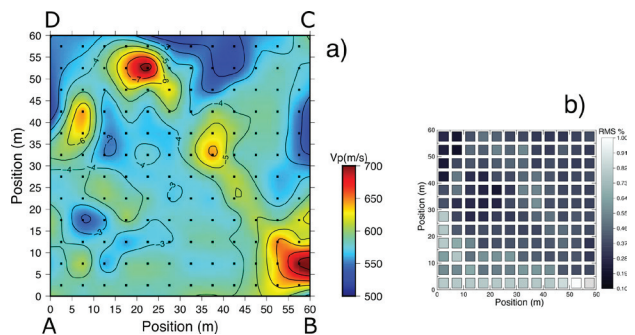


Figure 9. a) Pseudo seismic refraction tomography at Xalasco site. The black lines represent the iso-depths of the refractor layer in meters. Black dots are the centers of cells, b) RMS residuals representation of travel times inversion in each cell

DISCUSSION

The seismic refraction method makes it possible to determine the depth and velocity of a refractory layer reliably. The method resolution depends on the travel times identification of the refracted waves and the best fit to a subsoil inversion model (Palmer, 1981; Yilmaz, 2015). This study identified these travel times in two closed seismic arrays of sources and receivers. Thanks to the refraction method principle, it was possible to build tomography images showing the P-wave velocity distribution and the depth of the first refractive horizon. Constructing a tomography image of a second horizon requires considerable penetration energy produced

by the seismic source and a more excellent velocity contrast in depth. At the moment, the method resolution depends on the best line fit to travel times; however, this can be improved if an inversion procedure is incorporated (e.g., Sheehan *et al.*, 2005; Zelt *et al.*, 2013).

The RTSRS method results applied to two archaeological sites show evidence of the shape and elastic properties of the substratum. In the Casas Tapadas site, the irregularity in-depth and velocity values (Figure 8a) correspond to more sane materials found below the superficial layer shown in Figure 6a. The site is not precisely a sedimentary zone, where materials are usually deposited in horizontal layers. Instead, it is a volcanic zone where sedimentary materials may be alternated with extrusive igneous rocks (Pérez *et al.*, 1999; Morales *et al.*, 2015). Therefore, the results shown in Figure 8a indicate that filling materials were used to level the ground to construct the pyramidal base.

In the Xalasco site, seismic refraction sections (Figure 6a) also show the thickness of a thin layer that overlaps an irregular subsoil horizon with a slightly higher velocity. The filling layer can be associated with sedimentary materials where agricultural work is carried out. According to the topography, the area covered by the seismic array corresponds to a foreland (see the image in Figure 2b) where archaeologists infer the presence of a prehispanic basement. A first geophysical exploration of the presence of this basement was presented by López *et al.* (2016). These authors conducted two perpendicular lines (crossing the foreland center) of electrical resistivity tomography, whose results show a thin laterally discontinuous horizon of low resistivity (approximately 2 m thick). Therefore, we believe that the irregular velocity distribution (velocities greater than 600 m/s) shown in Figure 9a corresponds precisely to the remains of a Prehispanic andesitic basement described by López *et al.* (2016).

CONCLUSIONS

In this study, we have expanded the seismic refraction method, typically performed in a linear array of sources and receivers, to be used in a quadrangular array to obtain a depth image of the P-wave velocity subsurface. In addition, we applied the method to two archaeological sites, where it is necessary to explore the subsoil without invading the study area.

RTSRS results on the Plazuelas site show that the substratum is irregular with an inclination to the southern, reaching up to 7 m deep. This result is congruent with seismic refraction profiles, showing that the surface layer thickness increases from North to South. These observations support the archaeologists' conjecture

about the ground leveling for constructing a pyramidal base to expand the southern pyramid of Casas Tapadas.

At the Xalasco site, a weak velocity contrast between the surface and the underlying layers is observed. However, this contrast is enough to show the presence of anomalies could be associated with the remains of a Prehispanic andesitic basement (López *et al.*, 2016), materials, already evidenced in the surroundings by other geophysical methods and direct excavations (Juares *et al.*, 2017).

The identification and selection of refracted arrival times is a fundamental step to obtain an adequate pseudo tomography. Identifying these arrivals may be affected by material attenuation, velocity inversions, or a high cultural noise level if the study is carried out in an urban area. At the moment, this method does not allow detecting irregularities of layers close to the surface. However, the method can be enhanced with ambient seismic noise tomography or electrical tomography, techniques already developed by the Engineering School.

ACKNOWLEDGEMENT

This work was supported by UNAM-DGAPA projects: PAPIIT IN117119 and PAPIME PE105520. Thanks to the archaeologists Castañeda-López Carlos † and López-García Pedro Antonio of INAH for the invitation and facilitating the experiments realization in the sites of Plazuelas and Xalasco, respectively. We appreciate the comments and suggestions of three anonymous reviewers who improved the manuscript essence.

REFERENCES

- Aki, K. (1957). Space and time spectra of stationary stochastic waves, with special reference to microtremors. *Bulletin of the Earthquake Research Institute*, 35, 415-456.
- Argote-Espino, D. L., López-García, P. A., & Tejero-Andrade, A. (2016). 3D-ERT geophysical prospecting for the investigation of two terraces of an archaeological site northeast of Tlaxcala state, Mexico. *Journal of Archaeological Science: Reports*, 8, 406-415. <http://dx.doi.org/10.1016/j.jasrep.2016.06.047>
- Argote, D. L., Tejero-Andrade, A., Cárdenas-Soto, M., Cifuentes-Nava, G., Chávez, R. E., Hernández-Quintero, E., & Ortega, V. (2020). Designing the underworld in Teotihuacan: Cave detection beneath the moon pyramid by ERT and ANT surveys. *Journal of Archaeological Science*, 118, 105-141.
- Balestrini, F., Draganov, D., Malehmir, A., Marsden, P., & Ghose, R. (2020). Improved target illumination at Ludvika mines of Sweden through seismic-interferometric surface-wave suppression. *Geophysical prospecting*, 68(1-Cost-Effective and Innovative Mineral Exploration Solutions), 200-213.

- Brantley, S.L., White, T.S., White, A.F., Sparks, D., Richter, D., Pre-gitzer, K., Derry, L., Chorover, O., April, R., Anderson, S., & Amundson, R. (2006). Frontiers in exploration of the critical zone. National Science Foundation Workshop, October 24-26, 2005, Newark, USA.
- Cárdenas-Soto, M., Ramos-Saldaña, H., & Vidal-García, M. C. (2016). Interferometría de ruido sísmico para la caracterización de la estructura de velocidad 3D de un talud en la 3ª Sección del Bosque de Chapultepec, Ciudad de México. *Boletín de la Sociedad Geológica Mexicana*, 68(2), 173-186.
- Cárdenas-Soto, M., Escobedo-Zenil, D., Tejero-Andrade, A., Nava-Flores, M., Vidal-García, M. C., & Natarajan, T. (2020). Exploring a near-surface subsidence over a rehabilitated underground mine through ambient seismic noise tomography in combination with other geophysical methods. *Near Surface Geophysics*, 18(5), 483-495.
- Cárdenas-Soto, M., Piña-Flores, J., Escobedo-Zenil, D., Vidal-García, M. C., Natarajan, T., Hussain, Y., & Sánchez-Sesma, F. J. (2021). Seismic ambient noise tomography to retrieve near-surface properties in soils with significant 3D lateral heterogeneity: the case of Quinta Colorada building in Chapultepec, Mexico. *Natural Hazards*, 108, 129-145. <https://doi.org/10.1007/s11069-021-04735-4>
- Chávez-García, F. J., Natarajan, T., Cárdenas-Soto, M., & Rajendran, K. (2021). Landslide characterization using active and passive seismic imaging techniques: a case study from Kerala, India. *Natural Hazards*, 105(3), 1623-1642. <https://link.springer.com/article/10.1007/s11069-020-04369-y>
- Forghani, F., & Snieder, R. (2010). Underestimation of body waves and feasibility of surface-wave reconstruction by seismic interferometry. *The Leading Edge*, 29(7), 790-794. <https://doi.org/10.1190/1.3462779>
- Gámez-Lindoro, J.A. (2021). *Análisis de variaciones laterales de velocidad de onda sísmica utilizando tomografía sísmica con fuentes y receptores en superficie*. (Tesis de licenciatura). Facultad de Ingeniería, UNAM. México. Retrieved on <http://132.248.9.195/ptd2020/marzo/0801673/Index.html>
- García-Jerez, A., Luzón, F., Navarro, M., & Pérez-Ruiz, J. A. (2006). Characterization of the sedimentary cover of the Zafarraya basin, southern Spain, by means of ambient noise. *Bulletin of the Seismological Society of America*, 96(3), 957-967. <https://doi.org/10.1785/0120050061>
- Huerta-Hilario, N. (2017). *Prospección magnetométrica en la zona de Plazuelas, Guanajuato*. (Tesis de licenciatura). Facultad de Ingeniería, UNAM. México. Retrieved on <http://132.248.9.195/ptd2017/julio/0761760/Index.html>.
- Hellel, M., Oubaiche, E. H., Chatelain, J. L., Bensalem, R., Amarni, N., Boukhrouf, M., & Wathelet, M. (2019). Efficiency of ambient vibration HVSr investigations in soil engineering studies: backfill study in the Algiers (Algeria) harbor container terminal. *Bulletin of Engineering Geology and the Environment*, 78(7), 4989-5000. <https://doi.org/10.1007/s10064-018-01458-y>
- Hussain, Y., Cardenas-Soto, M., Martino, S., Moreira, C., Borges, W., Hamza, O., Prado R., Uagoda R., Rodríguez-Rebolledo J., Cerqueira-Silva R., & Martínez-Carvajal, H. (2019). Multiple geophysical techniques for investigation and monitoring of sobradinho landslide, Brazil. *Sustainability*, 11(23), 66-72. <https://doi.org/10.3390/su11236672>
- Juárez, K., López-García, P., Argote-Espino, D. L., Tejero-Andrade, A., Chávez, R. E., & García-Serrano, A. (2017). Magnetic and electrical prospecting in the archaeological site of Xalasco northeast of Tlaxcala, Mexico. *Global J. Archaeol. Anthropol.*, 2(2), 555-581. <https://doi.org/10.19080/GJAA.2017.02.555581>
- Kaminsky, A. (2015). ZondST2D (Software). Retrieved on May 18, 2020 on <http://zond-geo.com/english/>
- Lermo, J., & Chávez-García, F. J. (1994). Site effect evaluation at Mexico City: dominant period and relative amplification from strong motion and microtremor records. *Soil Dynamics and Earthquake Engineering*, 13(6), 413-423. [https://doi.org/10.1016/0267-7261\(94\)90012-4](https://doi.org/10.1016/0267-7261(94)90012-4)
- Liu, Y., Xia, J., Xi, C., Dai, T., & Ning, L. (2021). Improving the retrieval of high-frequency surface waves from ambient noise through multichannel-coherency-weighted stack. *Geophysical Journal International*, 227(2), 776-785. <https://doi.org/10.1093/gji/ggab253>
- López-García, P. A., Argote-Espino, D. L., & Tejero-Andrade, A. (2016). Informe del proyecto prospección arqueológica de los sitios de los Teteles de Ocotitla y Xalasco, Noreste de Tlaxcala. Temporada 2015. Archivo Técnico de la Coordinación Nacional de Arqueología, INAH, México.
- Manzanilla, L., & Bautista, J. A. (2009). Salvamento arqueológico en un conjunto con materiales teotihuacanos en Xalasco, Atlazayanca, Tlaxcala. *Boletín del Consejo de Arqueología*. INAH, México.
- Martorana, R., & Capizzi, P. (2020). Seismic and non-invasive geophysical surveys for the renovation project of Branciforte Palace in Palermo. *Archaeological Prospection*. <http://dx.doi.org/10.1002/arp.1781>
- Morales, J., Castañeda, C., García, E. C., & Goguitchaishvili, A. (2015). Nuevas evidencias sobre la edad de abandono del sitio arqueológico Plazuelas (Guanajuato, México) mediante la datación arqueomagnética de un piso quemado. *Arqueología Iberoamericana*, 7(28), 40-45.
- Nakamura, Y. (1989). A method for dynamic characteristics estimation of subsurface using microtremor on the ground surface. Railway Technical Research Institute, Quarterly Reports, 30(1), 25-33.
- Nazarian, S. (1984). *In situ determination of elastic moduli of soil deposits and pavement systems by spectral-analysis-of-surface-waves method*. (Tesis doctoral). University of Texas at Austin.
- Louie, J. N. (2001). Faster, better: shear-wave velocity to 100 meters depth from refraction microtremor arrays. *Bulletin of the Seismological Society of America*, 91(2), 347-364. <https://doi.org/10.1785/0120000098>

- Nazarian, S., & Desai, M. R. (1993). Automated surface wave method: field testing. *Journal of geotechnical engineering*, 119(7), 1094-1111. [https://doi.org/10.1061/\(ASCE\)0733-9410\(1993\)119:7\(1094\)](https://doi.org/10.1061/(ASCE)0733-9410(1993)119:7(1094))
- Palmer, D. (1981). An introduction to the generalized reciprocal method of seismic refraction interpretation. *Geophysics*, 46(11), 1508-1518. <https://doi.org/10.1190/1.1441157>
- Park, C. B., Miller, R. D., & Xia, J. (1999). Multichannel analysis of surface waves. *Geophysics*, 64(3), 800-808.
- Ramos-Román, G. (2015). *Tomografía sísmica por promedio de velocidades en 2D y 3D*. (Tesis de licenciatura). Facultad de Ingeniería, UNAM. México. Retrieved on <http://132.248.9.195/ptd2015/mayo/0729956/Index.html>
- Rocha-Jaime, J. M. (2017). *Búsqueda de vestigios arqueológicos, con estudio de georadar en 3D de la Zona Arqueológica de Plazuelas en Pénjamo Guanajuato*. (Tesis de licenciatura). Facultad de Ingeniería, UNAM. México. Retrieved on <http://132.248.9.195/ptd2017/noviembre/0768347/Index.html>.
- Okada, H., & Suto, K. (2003). *The microtremor survey method*. Society of Exploration Geophysicists.
- Pérez-Flores, E., Mauvois-Guitteaud, R., Menguelle-López, J., Moreno-Vázquez, J., Soto-Araiza, R., & López-Ojeda, J. (1999). Carta geológico-minera F14-10, Querétaro, escala 1:250000. Retrieved on https://mapserver.sgm.gob.mx/Cartas_Online/geologia/77_F14-10_GM.pdf
- Secretaría de Cultura/INAH (2020). (n.d.). Plazuelas. Retrieved on february 24 on https://sic.cultura.gob.mx/ficha.php?table=zona_arqueologica&table_id=175&estado_id=11
- Shapiro, N. M., & Campillo, M. (2004). Emergence of broadband Rayleigh waves from correlations of the ambient seismic noise. *Geophysical Research Letters*, 31(7). <https://doi.org/10.1029/2004GL019491>
- Shapiro, N. M., Nakata, N., Gualtieri, L., & Fichtner, A. (2019). Applications with surface waves extracted from ambient seismic noise. *Seismic Ambient Noise*, 218.
- Sheehan, J. R., Doll, W. E., & Mandell, W. A. (2005). An evaluation of methods and available software for seismic refraction tomography analysis. *Journal of Environmental & Engineering Geophysics*, 10(1), 21-34. <https://doi.org/10.2113/JEEG10.1.21>
- Williams, T., & Kelley, C. (2019). Gnuplot 5.2: an interactive plotting program (Software). Retrieved on <http://www.gnuplot.info/>
- Xia, J., Miller, R. D., & Park, C. B. (1999). Estimation of near-surface shear-wave velocity by inversion of Rayleigh waves. *Geophysics*, 64(3), 691-700.
- Yılmaz, Ö. (2015). *Engineering seismology with applications to geotechnical engineering*. Society of Exploration Geophysicists.
- Zelt, C. A., Haines, S., Powers, M. H., Sheehan, J., Rohdewald, S., Link, C., Hayashi, K.; Zhao, D.; Zhou, H.; Burton, B. L.; Petersen, U. K.; Bonal, N. D., & Doll, W. E. (2013). Blind test of methods for obtaining 2-D near-surface seismic velocity models from first-arrival traveltimes. *Journal of Environmental and Engineering Geophysics*, 18(3), 183-194. <http://dx.doi.org/10.2113/JEEG18.3.183>
- Cómo citar:**
Cárdenas-Soto, M., Gámez-Lindoro, J. A., Peña-Gaspar, V., Aguirre-Díaz, J. P. & García-Serrano, A. (2022). A Pseudo 3D Seismic Refraction Tomography for Exploring Archaeological Structures. *Ingeniería Investigación y Tecnología*, 23 (01), 1-9. <https://doi.org/10.22201/fi.25940732e.2022.23.1.003>